Use of a rapid human primary cell-based disease screening model, to compare next generation products to combustible cigarettes

Liam Simms [a,*], Elizabeth Mason [a], Ellen L. Berg [c], Fan Yu [a], Kathryn Rudd [a], Lukasz Czekala [a], Edgar Trelles Sticken [b], Oleg Brinster [b], Roman Wieczorek [b], Matthew Stevenson [a], Tanvir Walele [a]

[a] Imperial Brands PLC, 121 Winterstoke Road, Bristol BS3 2LL UK
[b] Reemtsma Cigarettenfabriken GmbH, An Imperial Brands PLC Company, Albert-EinsteinRing-7, D-22761 Hamburg, Germany
[c] Eurofins Discovery, Inc., 111 Anza Blvd, Suite 414, Burlingame, CA 94010, USA

ARTICLE INFO

ABSTRACT

A growing number of public health bodies, regulators and governments around the world consider electronic vapor products a lower risk alternative to conventional cigarettes. Of critical importance are rapid new approach methodologies to enable the screening of next generation products (NGPs) also known as next generation tobacco and nicotine products. In this study, the activity of conventional cigarette (3R4F) smoke and a range of NGP aerosols (heated tobacco product, hybrid product and electronic vapor product) captured in phosphate buffered saline, were screened by exposing a panel of human cell-based model systems using Biologically Multiplexed Activity Profiling (BioMAP® Diversity PLUS® Panel, Eurofins Discovery). Following exposure, the biological activity for a wide range of biomarkers in the BioMAP panel were compared to determine the presence of toxicity signatures that are associated with specific clinical findings. NGP aerosols were found to be weakly active in the BioMAP Diversity PLUS Panel (≤3/148 biomarkers) whereas significant activity was observed for 3R4F (22/148 biomarkers). Toxicity associated biomarker signatures for 3R4F included immunosuppression, skin irritation and thrombosis, with no toxicity signatures seen for the NGPs. BioMAP profiling could effectively be used to differentiate between complex mixtures of cigarette smoke or NGP aerosol extracts in a panel of human primary cell-based assays. Clinical validation of these results will be critical for confirming the utility of BioMAP for screening NGPs for potential adverse human effects.

Introduction

Cigarette smoking is a cause of serious disease including lung cancer, cardiovascular disease and emphysema. In recent years, a range of next generation products (NGPs) also known as next generation tobacco and nicotine products, have been developed. These products aim to deliver nicotine to the user, without burning tobacco and generating harmful tobacco smoke. The tobacco and nicotine harm risk continuum, is a concept introduced by McNeil and Munafo (2013), that ranks tobacco and NGPs according to their potential to cause harm, cigarettes are at the highest risk extreme and nicotine replace-ment therapy at the lowest (McNeill and Munafò, 2013). In order to be a viable tobacco harm reduction product and provide a benefit to public health, these products must (i) deliver nicotine in a comparable way to tobacco cigarettes (O'Connell et al., 2019), so that they are satisfying for adult smokers and facilitate transition away from smoking or reduce smoking and (ii) be scientifically demonstrated to be significantly less harmful than conventional cigarettes (Polosa et al., 2017; Walele et al., 2018). For example, electronic vapor products (EVPs) have been characterized by Public Health England as approximately 95% less harmful than conventional cigarettes (Farsalinos et al., 2013; McNeill et al., 2015) with recent research showing that EVPs

can assist adult smokers in replacing conventional cigarettes and reducing their cigarette per day consumption (Goniewicz et al., 2014; Misra et al., 2014). However, evidence potentially supporting the role of other novel tobacco containing NGPs such as heated tobacco products (HTPs) and hybrid devices (HYBs) in tobacco harm reduction is less advanced, due to the limited time of these products on the market.

The market for NGPs is rapidly expanding as adult smokers demand alternatives to tobacco cigarettes. For example, a 2014 study identified 7,764 different e-liquid flavor names, with 242 new flavors being added per month, and sales occurring under 466 brands (Zhu et al., 2014). Whilst HTPs have been available since the 1980′s, recent innovations are gaining popularity and this category of product is now available in 40 different countries (WHO, 2019). As such, there is a requirement for the development of standardized toxicity assessment screening methods that are cost effective and high throughput to support product stewardship, product development and commercialization of new products (Hartung, 2016). These assays need to be physiologically relevant for humans, capable of identifying potential toxicity likelihood, rapid to conduct and able to provide data for comparative studies.

The BioMAP® Diversity PLUS® Panel (Eurofins Discovery) consists of 12 human primary cell systems containing cell types from multiple tissues that represent a broad range of human biology, relevant to multiple diseases. The BioMAP cell systems are comprised of early passage human primary cell types cultured under conditions that model complex cellular regulatory signaling networks relevant to *in vivo* tissue states and human diseases (Houck et al., 2009; Kleinstreuer et al., 2014; Berg, 2017; O'Mahony, et al., 2018). They are in use as screening tools for drug development, repositioning of drugs, mechanism of action (MOA) insights, chemical safety assessments (ToxCast key partner (Kleinstreuer et al., 2014) and the determination of possible off target effects of generic drugs and pharmaceuticals (Berg, 2017). Primary cells are not immortalized and as such are closer to physiological cellular conditions in humans than immortalized cell lines. The 12 cell systems are cultured either as a single cell type or as co-cultures and stimulated with a combination of factors, such as cytokines, growth factors and mediators, to replicate the multi-component signaling networks associated with tissue and disease states. These signaling pathways are seen in healthy human cells under unstimulated conditions (Berg, 2017). Test article profiles were generated by measuring changes in the levels of 148 biomarker readouts (7 – 17 per system) following exposure. Biomarker readouts, primarily cell-surface proteins, have been validated using agents with known MOA. They include cell surface receptors, cytokines, chemokines, matrix molecules and enzymes. The proteins measured in this panel as cell-surface forms are expressed and their modulation by bioactive agents has been previously established (see Supplementary information). Each test article generates a signature profile that was created from the changes in protein biomarker readouts across the 12 cell systems. The biomarkers chosen were based on relevant disease-associated biomarkers measured in human clinical studies. There is some repetition of the biomarkers across the 12 cell systems to allow for comparison across systems.

The products investigated in this study were the Kentucky reference cigarette (3R4F), a HTP, a HYB and an EVP in the BioMAP Diversity PLUS assay. Trapping of cigarette smoke or NGP aerosol constituents in phosphate buffered saline (PBS) is a common exposure method amongst others (such as trapping using a Cambridge filter pad, in cell media or artificial saliva etc.) (Johnson et al., 2009). The trapped constituents can then be readily added directly to the cell systems. The use of smoke (from cigarettes) or aerosol (from HTP, HYP and EVP) bubbled directly through PBS, the resulting extract is termed bubbled PBS (bPBS). It has been previously demonstrated that cigarette smoke or NGP aerosol bPBS is able to trap water soluble fractions of smoke/aerosol. In addition, the use of trapped bPBS samples with

3D lung models, has shown that cigarette smoke delivery using bPBS give a good representation of absorption in the lungs as seen in the *in vivo* situation (Buratto et al., 2018; Mathis et al., 2013). We believed bPBS is a possible alternative vehicle compared to the use of total particulate matter (TPM) collected using a Cambridge filter pad (which excludes the trapping of the gas phase constituents), which has been used historically (Smart and Phillips, 2021). Nicotine has been routinely used as a marker of dosimetry/exposure in multiple studies both in cells, and animals and humans due to almost complete transfer into mainstream smoke/aerosol, its stability, and ease of measurement (Adamson et al., 2017; Behrsing et al., 2018). Nicotine is typically measured in human and animal blood as a marker of exposure (Benowitz et al., 2009). The aim of the study was to screen the aerosols from a range of commercially available NGPs, compared to that of cigarette smoke, using bPBS, then to assess the relative potential comparative risks of the different NGPs types when compared to conventional cigarettes in a human primary cell-based screening model. This assay is not a stand-alone assay but part of a wider series of assays and would be used as part of an overall weight of evidence approach.

Material and methods

Study products

The test samples used to generate smoke/aerosols are described in Table 1. All samples were purchased in 2018.

The 3R4F cigarettes were stored at 4 °C in an airtight container and prior to use were equilibrated to room temperature for 15 min before conditioning of both 3R4F and HTP sticks in a standard humidified chamber or at least 48 h, according to the International Organization for Standardization (ISO) Guideline 3402 (ISO, 1999). Both the EVP and HYB pods were stored at room temperature until use, and all battery powered devices were fully charged before use.

Smoke / aerosol extract generation method

Cigarette (3R4F) smoke and EVP, HYB and HTP aerosols were generated using a Vitrocell VC 10S-Type smoking machine (Vitrocell, Waldkirch, Germany). The cigarette smoke or NGP aerosol was extracted by bubbling through three in-line impingers each containing 10 mL of PBS solution (Sigma-Aldrich, Germany) at room temperature, resulting in a total sample stock volume of 30 mL. The Vitrocell VC 10S-type smoking port was directly linked to the impingers, therefore there was no cigarette smoke or NGP aerosol dilution during test article generation. Cigarette smoke and NGP aerosols were generated according to Table 2. For 3R4F we used: 6 cigarettes with 9 puffs each;

Table 1

Test samples evaluated in the BioMAP Diversity PLUS panel.

Sample	Product category	Coding	Source
Kentucky 3R4F reference cigarette	Cigarette	3R4F	University of Kentucky (Batch No. V062X53D)
IQOS with Amber HEETs	Heated tobacco product	HTP	Philip Morris International German market
iFuse with Kent Neopods 109, 1.8 % nicotine	Hybrid product	HYB	British American Tobacco Romanian market
*my*blu[1] with tobacco flavour, 1.6%[w/w] nicotine[2]	Electronic vapour product cigarette	EVP	Fontem Ventures UK market

[1] The *my*blu™ is a closed pod-system EVP, consisting of two segments (a rechargeable battery section (350mAh battery capacity) and a replaceable pod containing e-liquid (1.5 mL; 1.3 Ω coil resistance).

[2] The *my*blu e-liquid was made by a subsidiary of Imperial Brands PLC, for research purposes only.

Table 2
Smoke/aerosol production parameters.

Test Sample	Smoking regime	Puff volume (mL)	Puff duration (s)	Puff interval (s)	Number of puffs	Ventilation blocking	Puff profile	Smoking machine
3R4F	ISO:20778:2018 (Standardization, 2018a)	55	2	30	54	Yes	Bell	Rotary
HTP	ISO:20778:2018 (Standardization, 2018a)	55	2	30	120	N/A	Bell	Rotary
HYB	ISO:20768:2018 (Standardization, 2018b)	55	3	30	120	N/A	Square	Rotary
EVP	ISO:20768:2018 (Standardization, 2018b)	55	3	30	120	N/A	Square	Rotary

Puff profiles are bell shaped, or square wave to allow for heating of the element (HYB and EVP)

For HTP: 12 devices, with one stick per device, and 10 puffs per stick; HYB: 2 devices, with one pod per device and 60 puffs each and EVP: 2 devices, with one pod per device and 60 puffs each. For both the EVP and HYB, 60 puffs were used on each device, the recommended number of puffs for each pod is stated to be approximately 150 puffs for EVP and 200 puffs for the HYB, to ensure there was ample product left during testing.

All experimental runs took 30 min. Aliquots were frozen in less than 5 min after generation. Aliquots were then stored at −70 °C and shipped to Eurofins Discovery on dry ice.

Bubbled PBS characterization

Nicotine and eight selected carbonyls, based on the list described by Buratto et al. (2018), were quantified within the aerosol and smoke bPBS samples. Methodology as previously described by Simms et al. (2020) and Czekala et al. (2021)). In brief, nicotine was quantified using liquid chromatography with tandem mass spectrometry (LC-MS/MS) with an AB Sciex API 6500 QTRAP (SCIEX, Framingham, MA, USA). Carbonyl detection methodology in bPBS was adapted from ISO 21160:2018 (ISO, 2018) methodology for carbonyl detection. Carbonyl-DNPH derivates, were quantified using high-performance liquid chromatography with a diode-array detector (HPLC-DAD, Agilent Technologies 1100 Series, Agilent Technologies, Santa Clara, CA, USA).

Cell systems and culture

The cell systems and biomarker readouts of the BioMAP Diversity PLUS panel are presented in Table 3. Detailed methods for the panel can be found in Shah et al. (2017) and Supplemental Methods (Shah et al., 2017).

Cell types and stimuli used in each system are as previously published (Shah et al., 2017) and follows: 3C system [Human umbilical vein endothelial cells (HUVEC) + (IL-1β, TNFα and IFNγ)], 4H system [HUVEC + (IL-4 and histamine)], LPS system [Peripheral blood mononuclear cells (PBMC) and HUVEC + LPS (Toll-like receptor (TLR) 4 ligand)], SAg system [PBMC and HUVEC + T cell receptor (TCR) ligands], BT system [CD19 + B cells and PBMC + (α-IgM and TCR ligands)], BF4T system [bronchial epithelial cells and Human neonatal dermal fibroblasts (HDFn) + (TNFα and IL-4)], BE3C system [bronchial epithelial cells + (IL-1β, TNFα and IFNγ)], CASM3C system [coronary artery smooth muscle cells + (IL-1β, TNFα and IFNγ)], HDF3CGF system [HDFn + (IL-1β, TNFα, IFNγ, EGF, bFGF and PDGF-BB)], KF3CT system [keratinocytes and HDFn + (IL-1β, TNFα, IFNγ and TGFβ)], MyoF system [differentiated lung myofibroblasts + (TNFα and TGFβ)] and /Mphg system [HUVEC and M1 macrophages + Zymosan (TLR2 ligand)].

Human primary cells in BioMAP systems are used at early passage (passage 4 or earlier) to minimize adaptation to cell culture conditions and preserve physiological signaling networks. All cells are from multiple donors (n = 2–6), commercially purchased, handled according to the recommendations of the manufacturers and pooled before assay. Human blood derived CD14 + monocytes are differentiated into macrophages *in vitro* before being added to the Mphg system.

Systems are derived from either single cell types or co-culture systems. Adherent cell types are cultured in 96 or 384-well plates until confluence, and optionally followed by the addition of peripheral blood mononuclear cells, PBMC (added to SAg and LPS systems only). The BT system consists of CD19 + B cells co-cultured with PBMC and stimulated with a B-cell receptor activator and low levels of TCR stimulation.

Endpoint measurements

For profiling in the BioMAP Diversity PLUS panel, we followed the standard format from Eurofins Discovery. For screening purposes all test articles were evaluated at 4 concentrations in singlicate across 148 assay endpoints. The BioMAP assay panels have been standardized and in commercial operation for > 10 years and data on reproducibility has been previously published (Houck et al., 2009; Kleinstreuer et al., 2014).

All bPBS samples were well mixed prior to dosing and tested at 0.12%, 0.25%, 0.5% and 1%. Test articles were added at the indicated concentrations 1-hr before stimulation, and remained in culture for 24-hrs, except for the MyoF system (48-hrs) and BT system (72-hrs for soluble readouts and 168-hrs for secreted IgG). Each plate contained positive controls (colchicine at 1.1 μM), negative controls (e.g., non-stimulated conditions) and vehicle controls (e.g., 0.1% DMSO) appropriate for each of the 12 cell systems.

Overt adverse effects of test articles on cell proliferation and viability (cytotoxicity) were detected by protein staining with sulforhodamine B (SRB) or alamarBlue® reduction for cells in suspension. Cytotoxicity for adherent cells was measured at time points optimized for each system (24-hrs: 3C, 4H, LPS, SAg, BF4T, BE3C, CASM3C, HDF3CGF, KF3CT, and /Mphg systems; 48-hrs: MyoF system). Proliferation of adherent cell types was quantified by SRB staining. Individual cell types were cultured at subconfluence and measured at time points optimized for each system (48-hrs: 3C and CASM3C systems; 72-hrs: BT and HDF3CGF systems; 96-hrs: SAg system). Proliferation of PBMC (T cells) was quantified by alamarBlue® reduction (24-hrs: SAg system; 42-hrs: BT system).

The levels of biomarker readouts were measured by enzyme-linked immunosorbent assay (ELISA), as previously described (Shah et al., 2017) and in Supplemental Methods.

Data analyses

Biomarker measurements in a test article-treated sample were divided by the average of control samples (at least 6 vehicle controls from the same plate) to generate a ratio that was then log_{10} transformed. The significance prediction envelopes were calculated using

Table 3
BioMAP systems and readouts (Plus, 2021).

System	Relevance	Cell type	Biomarker Readout
/Mphg	Cardiovascular Disease, Chronic Inflammation, Restenosis	Macrophages + HUVECs	CCL2/MCP-1, CCL3/MIP-1 α, CD106/VCAM-1, CD40, CD62E/E-Selectin, CD69, CXCL8/IL-8, IL-1 α, M−CSF, sIL-10, SRB, SRB-Mphg
3C	Cardiovascular Disease, Chronic Inflammation	HUVECs	CCL2/MCP-1, CD106/VCAM-1, CD141/Thrombomodulin, CD142/Tissue Factor, CD54/ICAM-1, CD62E/E-Selectin, CD87/uPAR, CXCL8/IL-8, CXCL9/MIG, HLA-DR, Proliferation, SRB
4H	Allergy, Asthma, Autoimmunity	HUVECs	CCL2/MCP-1, CCL26/Eotaxin-3, CD106/VCAM-1, CD62P/P-Selectin, CD87/uPAR, SRB, VEGFR2
BE3C	Chronic obstructive pulmonary disease (COPD), Lung Inflammation	Bronchial epithelial cells	CD54/ICAM-1, CD87/uPAR, CXCL10/IP-10, CXCL11/I-TAC, CXCL8/IL-8, CXCL9/MIG, EGFR, HLA-DR, IL-1 α, Keratin 8/18, MMP-1, MMP-9, PAI-I, SRB, tPA, uPA
BF4T	Allergy, Asthma, Fibrosis, Lung Inflammation	Bronchial epithelial cells + Dermal fibroblasts	CCL2/MCP-1, CCL26/Eotaxin-3, CD106/VCAM-1, CD54/ICAM-1, CD90, CXCL8/IL-8, IL-1 α, Keratin 8/18, MMP-1, MMP-3, MMP-9, PAI-I, SRB, tPA, uPA
BT	Allergy, Asthma, Autoimmunity, Oncology	B cells + Peripheral blood mononuclear cells	B cell Proliferation, PBMC Cytotoxicity, Secreted IgG, sIL-17A, sIL-17F, sIL-2, sIL-6, sTNF-α
CASM3C	Cardiovascular Inflammation, Restenosis	Coronary artery smooth muscle cells	CCL2/MCP-1, CD106/VCAM-1, CD141/Thrombomodulin, CD142/Tissue Factor, CD87/uPAR, CXCL8/IL-8, CXCL9/MIG, HLA-DR, IL-6, LDLR, M−CSF, PAI-I, Proliferation, Serum Amyloid A, SRB
HDF3CGF	Chronic Inflammation, Fibrosis	Dermal fibroblasts	CCL2/MCP-1, CD106/VCAM-1, CD54/ICAM-1, Collagen I, Collagen III, CXCL10/IP-10, CXCL11/I-TAC, CXCL8/IL-8, CXCL9/MIG, EGFR, M−CSF, MMP-1, PAI-I, Proliferation_72hr, SRB, TIMP-1, TIMP-2
KF3CT	Dermatitis, Psoriasis	Dermal fibroblasts + Keratinocytes	CCL2/MCP-1, CD54/ICAM-1, CXCL10/IP-10, CXCL8/IL-8, CXCL9/MIG, IL-1 α, MMP-9, PAI-I, SRB, TIMP-2, uPA
LPS	Cardiovascular Disease, Chronic Inflammation	Peripheral blood mononuclear cells + HUVECs	CCL2/MCP-1, CD106/VCAM-1, CD141/Thrombomodulin, CD142/Tissue Factor, CD40, CD62E/E-Selectin, CD69, CXCL8/IL-8, IL-1 α, M−CSF, sPGE2, SRB, sTNF-α
MyoF	Chronic Inflammation, Fibrosis, Matrix Remodeling, Wound Healing	Lung fibroblasts	bFGF, CD106/VCAM-1, Collagen I, Collagen III, Collagen IV, CXCL8/IL-8, Decorin, MMP-1, PAI-I, SRB, TIMP-1, α-SM Actin
SAg	Autoimmune Disease, Chronic Inflammation	Peripheral blood mononuclear cells + HUVECs	CCL2/MCP-1, CD38, CD40, CD62E/E-Selectin, CD69, CXCL8/IL-8, CXCL9/MIG, PBMC Cytotoxicity, Proliferation, SRB

the historical vehicle control data at a 95% confidence interval. Significance prediction envelopes were calculated for historical controls (95%). Included on every plate are 6–8 vehicle control samples (e.g., DMSO vehicle controls). Log_{10} ratio values (Log_{10} transformation of the ratio of measurement values in a single vehicle control well compared to the average of the plate vehicle controls) are calculated and have been collected over time (>3 years, >100 experiments) to generate a historical envelope of negative control values. The 95% significance envelope is the symmetrical upper and lower bound values of 95% of historical vehicle controls.

Profile analysis

Biomarker activities were annotated when the data from the sample at 2 or more consecutive concentrations changed in the same direction relative to vehicle controls outside of the significance envelope and had at least one concentration with an effect size > 20% ($|log_{10}$ $ratio|$ > 0.1). Biomarker key activities were described as modulated if these activities increased in some systems but decreased in others. Cytotoxic conditions were noted when total protein levels decreased by >50% (log_{10} $ratio$ values of SRB or alamarBlue < −0.3). A test article was considered to have broad cytotoxicity when cytotoxicity was detected in 3 or more systems. Concentrations of test articles with detectable broad cytotoxicity were excluded from biomarker activity annotations and further analyses. Antiproliferative effects were defined by an SRB or alamarBlue $|log_{10}$ $ratio|$value < −0.1 from cells plated at a lower density. Annotation of cytotoxicity and antiproliferative effects only required one concentration to be considered as such.

Benchmark analysis

Common biomarker readouts were identified when the readout measurement (Log_{10} ratio) for both profiles was outside of the significance envelope with an effect size > 20% in the same direction. Differentiating biomarkers were identified when one profile had a readout measurement value outside of the significance envelope with an effect size > 20%, and the readout measurement for the other profile was either inside the envelope or in the opposite direction. Unless specified, the top non-cytotoxic concentration of both the test article

and benchmark agent were included in the benchmark overlay analysis.

Toxicity signature analysis

Using data mining of a large reference database containing the results for drugs, experimental chemicals and other agents profiled in BioMAP systems, (>4500 compounds), Eurofins Discovery has revealed mechanisms of toxicity associated with human adverse effects reported during clinical trials. The subsequent development of these as toxicity signatures were considered to aid in understanding the mechanisms of toxicity of environmental chemicals (Berg et al., 2019) and could be applied to complex mixtures.

Nine toxicity signatures from BioMAP profiles exist for the following adverse events seen in human clinical trials; acute toxicity, immunosuppression, skin irritation, liver toxicity, organ toxicity, skin rash (MEK-related), skin sensitization, thrombosis-related side effects and vascular toxicity (Berg, 2019). These signatures (key biomarkers) are qualified for their association with the specific adverse events by using both statistical and biological plausibility criteria (for example, association of a key endpoint as a previously established clinical biomarker for the adverse effect). The BioMAP Reference Database of profiles for > 4000 test articles were used to test the strength of each association. Each toxicity signature consists of 2–5 individual biomarkers and data from known reference compounds that have a well-defined specific MOA. To determine toxicity signatures, original BioMAP Diversity PLUS data for 3R4F and NGPs was reanalyzed to look for alterations of the key biomarkers associated with each of the 9 toxicity signatures.

Toxicity Signatures were carried out at concentrations that were lower than those that caused overt cytotoxicity in the BioMAP systems, this is because cytotoxicity is not the most informative endpoint for most of the *in vivo* toxicity associations. Nearly all of the Toxicity Signatures developed from the BioMAP reference data are associated with biological processes that are not related to overt cell cytotoxicity. Only the signature for "Acute Toxicity" includes cytotoxicity-related endpoints (reduction in total protein measured by SRB/alamar blue of

> 50% in at least 3 cellular systems). See Berg (2019) for details of the other Toxicity Signatures.

Results

Characterization of bubbled PBS

Nicotine and eight carbonyls were detected following capture of the 3R4F bPBS. This puff count for 3R4F was approximately half the dose of the other NGPs (54 puffs vs 120 puffs of the NGPs). The use of 54 puffs of 3R4F was based on the toxicity of 3R4F seen in another study using whole smoke (Czekala et al., 2019). EVP delivered the most nicotine (152 ug/mL) but contained no detectable carbonyls (LOQ 0.5–1.5 μg/mL). As expected, carbonyl levels were the highest in 3R4F and HTP bPBS. Limited carbonyls were detected in HYB bPBS and none in EVP bPBS (See Table 4).

A 1-year preliminary stability study (data not shown) was conducted with the bPBS samples stored at −70 ˚C. It was found that after a year of storage there was a decrease of nicotine to 85% for the EVP sample only, the majority of the carbonyls did not change, however, there was a loss of highly reactive acrolein, with approximately 35% of fresh values remained in the 3R4F and non-detected in the HTP sample; crotonaldehyde dropped to 75% of the fresh values in the 3R4F and HTP samples. This indicated general stability for most carbonyls during storage at −70 ˚C for up to a year. Samples were generated and analyzed at DiscoverX within 6 weeks of generation, to minimize any possible loss of volatile carbonyls. Taylor et al. (2020) reported nicotine stability for up to 31 weeks in aqueous extracts of 3R4F, the maximal length of the study, no other analytes were determined (Taylor et al., 2020). Further work will look at the carbonyl stability of bPBS samples over shorter time points.

Dosimetry

Based on the volumes of bPBS liquid added to the individual Bio-MAP cell cultures (200 μL), dosed at the top concentration of 1% doses in terms of nicotine delivery ranged between 530 ng/mL (HYB) to 1520 ng/mL (EVP) and 64 to 183 ng/mL at the 0.12% concentration. Nicotine has typically been used to for the quantification of exposure in cigarettes and NGPs due to its high transfer rates and stability (Adamson et al., 2017; Behrsing et al., 2018). Typical peak nicotine concentrations after smoking a cigarette are 10–35 ng/mL of plasma (Schneider et al., 2001); whilst for EVPs and HTPs nicotine plasma concentrations reach 12 ng/mL EVP (O'Connell et al., 2019) and 9–12 ng/mL respectively (Brossard et al., 2017). The doses used for BioMAP profiling were above physiologically measured relevant levels in human plasma and therefore considered to be more of an extreme human use/worst case scenario being between 2 and 152 times higher than human measured levels.

Cellular effect of tested articles in BioMAP systems

Table 5 summarizes test article bioactivities in the BioMAP Diversity PLUS panel, including cytotoxicity, antiproliferative effects and the number of annotated biomarkers with their physio- and pathological relevance. A summary of the changes (increase, decrease) in biomarker readouts for all test articles are presented in Table 6. Experimental data on all test articles is included in Supplemental Table 3.

3R4F bPBS was active in the BioMAP Diversity PLUS panel with 20 annotated readouts in 7 cell systems. It was not cytotoxic to any human primary cell types at the tested concentrations (up to 1% bPBS added to the cell media) but was antiproliferative in four cell systems: B cells (1 %), T cells (1%, 0.5%), coronary artery smooth muscle cells (1%), and fibroblasts (1%, 0.5%) (Fig. 1A). 3R4F impacted inflammation-related activities, immunomodulatory activities, tissue remodeling activities, and haemostasis-related activities. Annotated biomarkers showed both decreases and increases in levels, dependent on the cell system. Tissue factor (TF) was increased in 3C and LPS cell systems. PGE2 was elevated in LPS, EGFR in HDF3CGF, IL8 in MyoF, and IL8 and IL-1α were elevated in the /Mphg cell system. VCAM −1 was decreased in LPS and HDF3CGF systems whereas CD40 was decreased in LPS and /Mphg systems.

In contrast to 3R4F, HTP, HYB and EVP bPBS were modestly active in the BioMAP Diversity Plus Panel with a limited number of biomarkers annotated and restricted to one to three cell systems (Fig. 1 B – D). All concentrations remained within close proximity to the control envelope (indicated by grey shading around the x-axis origin in the graph). At the concentrations tested, none of the NGPs showed cytotoxicity to cell types in any of the cell systems under the conditions of test, nor were they antiproliferative in any of the 12 cell systems when tested at concentrations up to 1%. For 3R4F and HYB there was an increase in EGFR for HDF3CGF (dermal fibroblasts), with a small decrease in EGFR seen for HTP and EVP with HDF3CGF and an increase in sil10 for HTP and EVP compared to a decrease seen for 3R4F for Mphg (HUVECs and macrophages). For HTP there was also a small decrease in macrophage colony-stimulating factor (M-CSF) in (CASM3C, coronary artery smooth muscle cells) and a decrease in Col-1 in HDF3CGF for EVP.

Toxicity signatures

Toxicity Signature Analysis of the Diversity PLUS panel data for each product were performed across all the concentrations used (0.12–1% bPBS, see Figure 2). No toxicity signatures were detected for any of the NGP products (HTP, HYB and EVP) under the conditions of test. 3R4F was the only product for which toxicity signatures could be identified (see Fig. 1A, Table 6); the toxicity signatures for immunosuppression and skin irritation were detected at concentrations ≥ 0.2 5%, and the signature for thrombosis was detected at the lowest concentration tested ≥ 0.12%. Note that at higher concentrations of 3R4F

Table 4
Nicotine and carbonyl quantification in pooled bPBS samples.

Concentration (μg/mL)	3R4F	HTP	HYB	EVP	LOQ (μg/mL)
Nicotine	82.5	123.0	53.0	152.0	0.01
Formaldehyde	5.9	0.9	1.0	<LOQ	0.25
Acetaldehyde	157.1	52.9	<LOQ	<LOQ	1.5
Acetone	24.0	5.4	<LOQ	<LOQ	1.0
Acrolein	9.4	1.3	0.5	<LOQ	0.5
Propionaldehyde	9.5	3.5	<LOQ	<LOQ	0.5
Crotonaldehyde	6.2	0.6	<LOQ	<LOQ	0.5
2-Butanone (MEK)	6.3	1.3	<LOQ	<LOQ	0.5
n-Butyraldehyde	3.6	2.8	<LOQ	<LOQ	0.5

LOQ = Limit of quantification

Table 5
Summary of cellular effects of tested articles in BioMAP systems.

Test Article	Cytotoxicity: System (Concentration)	Antiproliferative effects: Cell type	Annotated biomarkers (at non-cytotoxic concentrations)	Physio- and pathological relevance
3R4F	None	B cells Coronary artery smooth muscle cells Endothelial cells Fibroblasts	10	Inflammation-related activities Immunomodulatory activities
HTP	None	None	3	Immunomodulatory activities Tissue remodeling activities
HYB	None	None	1	Tissue remodeling activities
EVP	None	None	3	Immunomodulatory activities Tissue remodeling activities

Table 6
Cigarette and NGP activities in the BioMAP platform. Changes in key biomarker activities are listed by biomarker and biological disease classifications.

Biological and disease relevance activity	Decreased biomarker activity	Increased biomarker activity	Modulated activity*
3R4F			
Inflammation-related activities	MIP-1, sTNFα, VCAM-1, Eot3	sPGE2, IL-1α, IL-8	–
Immunomodulatory activities	M−CSF, sIL-10, sIL-2, sIL-6, CD40, sIL-17A	–	–
Tissue remodeling activities	–	EGFR	–
Haemostasis-related activities	–	TM, TF	–
HTP			
Immunomodulatory activities	M−CSF	sIL-10	–
Tissue remodeling activities	EGFR	–	–
HYB			
Tissue remodeling activities	–	EGFR	–
EVP			
Immunomodulatory activities	–	sIL-10	–
Tissue remodeling activities	EGFR, Col-I	–	–

*Biomarker key activities were described as modulated if these activities increased in some systems but decreased in others.

TPM, eluted with DMSO, additional signatures were identified (see Supplementary Figs. 1 and 2).

Discussion

The application of rapid, novel *in vitro* toxicity screening tests/assays are aligned with the principles of the 3R's and with the National Research Council (NRC) paper 'Toxicity Testing in 21st the Century' and subsequent documents (National Academies of Sciences et al., 2017; Krewski et al., 2010). The NRC vision calls for a move away from animal testing that is costly, slow, and of limited relevance to humans, in favor of *in vitro* use of human-derived cells and high throughput and omics technologies to look at the perturbation of key cellular signaling networks (Sheldon and Cohen Hubal, 2009).

The commercially available BioMAP phenotypic profiling platform has been used to analyze > 800 environmental chemicals as part of the U.S. Environmental Protection Agency ToxCast Program (Houck et al., 2009; Kleinstreuer et al., 2014), it has also been used to look at complex mixtures (Wetmore et al., 2019). The assay platform was able to reproducibly identify potential toxicities and off-target drug effects, as well as pinpoint cellular mechanisms and biomarkers underlying specific types of adverse reactions in humans (Kleinstreuer et al., 2014). The BioMAP panel uses a reference database built with data from > 4500 reference agents, including approved and failed drugs, chemicals, biologics, food additives and other materials. Comparative analysis of the BioMAP profiles of test articles with the ones of known bioactive compounds allows the identification of phenotypically similar compounds and provides insights into cellular targets, possible MOAs and safety across diverse physiological systems (Berg, 2019; Berg et al., 2013). Further analysis of the BioMAP profiles for the presence of toxicity-associated signatures uses the resulting biomarker profiles and profiles of known reference compounds held in the BioMAP database. This analysis determines the presence of profile characteristics (specific biomarkers alterations) within the BioMAP Diversity PLUS panel that are part of a defined signature associated with increased risk of certain adverse effects *in vivo*.

In this study, we used the BioMAP Diversity PLUS Panel, to characterize and screen the biological activities of 3R4F bPBS, and aerosol bPBS from a commercially available HTP, HYB and EVP. To our knowledge, this is the first study reporting the application of this system for the characterization of complex mixtures of tobacco and nicotine products. Our study endpoints included the impact of test articles on cytotoxicity, antiproliferative activity and the alteration of levels of a total of 148 biomarker readouts, primarily proteins, including both cell surface and secreted proteins. This BioMAP dataset was then used to identify the presence of BioMAP Toxicity Signatures, defined as sets of biomarker changes associated with clinical toxicity in reference compounds tested in humans.

Our results indicate that this *in vitro* assay platform could effectively be used to screen conventional cigarettes and NGPs in a highly relevant panel of human cell-based assays and be used as part of the weight of evidence approach with other *in vitro* assays to look at the
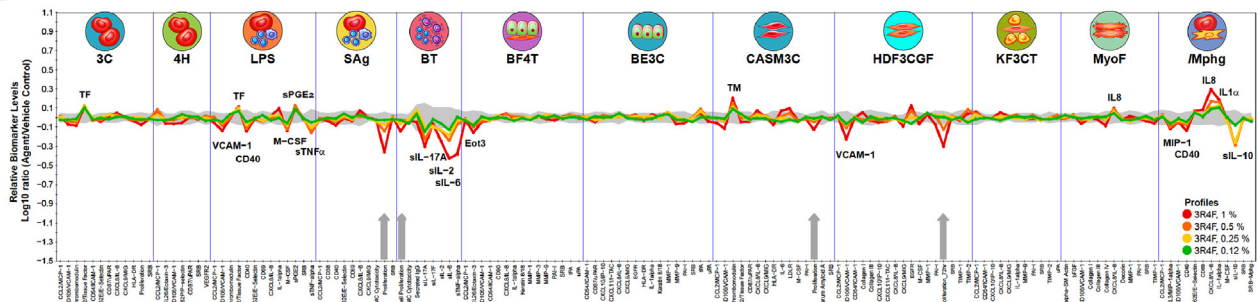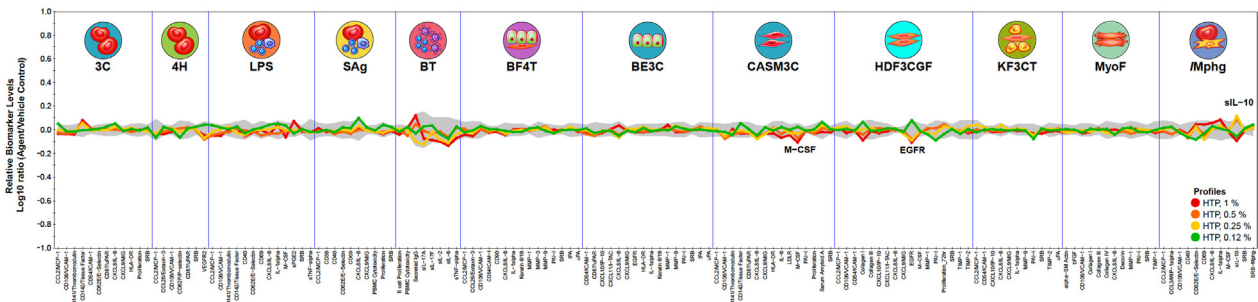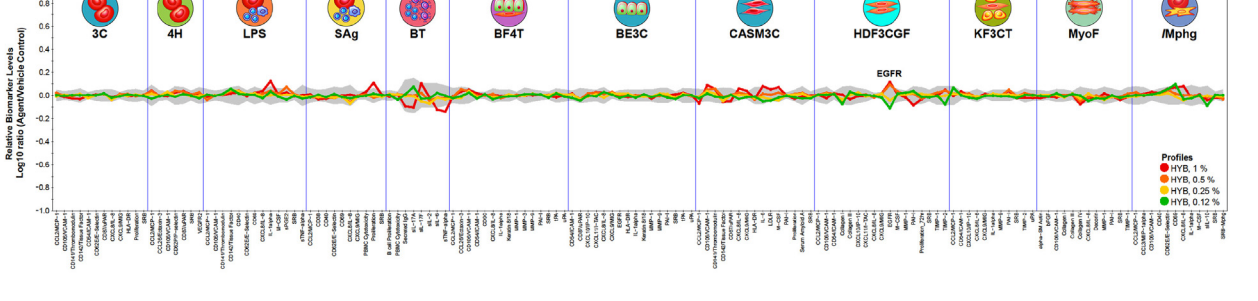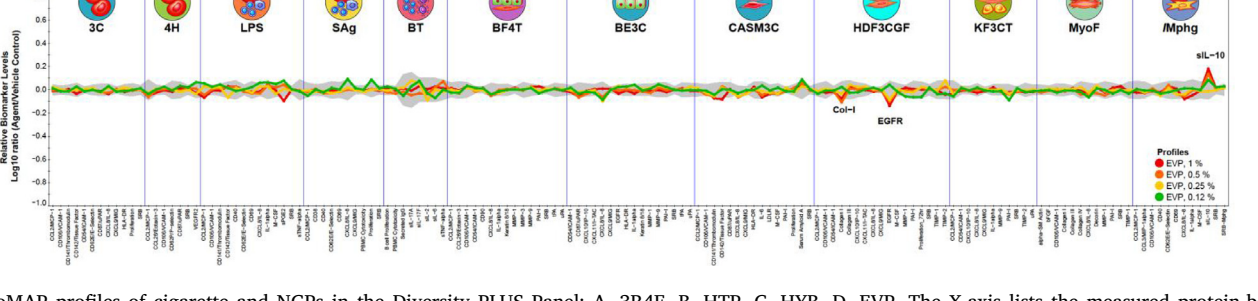
Fig. 1. BioMAP profiles of cigarette and NGPs in the Diversity PLUS Panel: A. 3R4F, B. HTP, C. HYB, D. EVP. The X-axis lists the measured protein-based biomarker readouts in each system. The Y-axis represents a log$_{10}$-transformed ratio of the biomarker readouts for the test article-treated sample (n = 1) over vehicle controls (n ≥ 6). The grey region around the Y-axis represents the 95% significance envelope generated from historical vehicle controls. Antiproliferative effects are indicated on the profile plot by thick grey arrows above the X-axis. Where the biomarker changes at 2 or more concentrations and follow the same directional trend they are annotated on the chart with grey arrows. Line colors indicate different test concentrations.

Test Agent	Acute Toxicity	Immuno-suppression	Skin Irritation	Liver Toxicity	Organ Toxicity	Skin Rash (MEK-related)	Skin Sensitization	Thrombosis	Vascular Toxicity
3R4F bPBS	ND	>=0.25%	>=0.25%	ND	ND	ND	ND	>=0.12%	ND
HTP bPBS	ND	ND	ND	ND	ND	ND	ND	ND	ND
HYP bPBS	ND	ND	ND	ND	ND	ND	ND	ND	ND
EVP bPBS	ND	ND	ND	ND	ND	ND	ND	ND	ND

Fig. 2. Toxicity Signature Analysis for the Diversity PLUS panel. Evaluation of the presence of Toxicity Signatures within the BioMAP profile of the tested article and concentrations detected. Toxicity Signatures are made up of 2–5 biomarker activities that have been correlated to an increased risk of certain toxicity effects *in vivo*. Concentrations are listed if the signature for the toxicity was detected. Not detected (ND) indicates the signature was not detected at any of the concentrations tested.

potential harm reduction potential of NGPs when compared to cigarettes. The identification of altered biomarkers could also be compared in future to data from clinical studies with human volunteers with identical products to assess the accuracy of the *in vitro* test system.

Test articles

This study used PBS to trap water soluble constituents of the cigarette smoke and NGP aerosols. In the case of this study, 120 puffs were collected from each NGP allowing for comparison either on a per puff or mL bPBS basis. For the 3R4F reference cigarette, less puffs were collected (54 puffs). This is due to the (cyto)toxicity observed for this product extract. For all test articles, nicotine was captured and quantified in the bPBS. This same trapping methodology and puff number has been used across a wide battery of assays, and responses have been observed for certain endpoints including the devTOX quickPredict assay (Simms et al., 2020).

It should be noted that is possible for particulate matter to be trapped in the PBS sample for the 3R4F due to the formation of carbon compounds from the combustion of tobacco (Pratte et al., 2017). Cigarette smoke is known to contain over 7000 different chemicals with HTP, HYB and EVP producing far fewer types of compounds due to the lack of combustion of these products (Pratte et al., 2017; Gasparyan et al., 2018). There are fundamental differences in the smoke/aerosol generated from the test products. For pre-clinical testing of NGP products, there is no standardized collection methodology of product aerosol. A recent review found the bubbling of cigarette smoke or NGP aerosol through an aqueous solvent was the predominant trapping methodology for *in vitro* testing of EVP aerosol (Smart and Phillips, 2021). Other collection methods, including TPM/aerosol collected mass (ACM) captured on a Cambridge filter pad and desorbed with DMSO could be used in the assay. Although TPM and ACM trapping is frequently employed for *in vitro* studies, this trapping methodology also has significant limitations. One possible limitation of this capture method is that aerosol/gas phase constituents are not retained by the Cambridge filter pad and are not collected (Smart and Phillips, 2021). The use of TPM/ACM with DMSO limits the amount of material you add due to toxicity of DMSO.

Cytotoxicity and antiproliferative effects

In this panel of assays, none of the products tested were cytotoxic to any of the cell systems up to the maximum concentrations tested of 1% added bPBS. The doses were deliberately chosen to be non-cytotoxic. In the BioMAP platform, cytotoxicity is not the most informative endpoint for most of the *in vivo* toxicity associations. Nearly all of the Tox-

icity Signatures developed from the BioMAP reference data are associated with biological processes that are not related to overt cell cytotoxicity. Only the signature for "Acute Toxicity" includes cytotoxicity-related endpoints (reduction in total protein measured by SRB or alamarBlue of >50% in at least 3 cellular systems). See Berg (2019) for details of the other Toxicity Signatures (Berg, 2019). For the other Toxicity Signatures, the presence of cytotoxicity masked their detection.

Given that the concentrations of the test article bPBS caused overt cytotoxicity and were above their estimated *in vivo* exposures (See Dosimetry section in results), it was thought possible that at a lower, non-cytotoxic concentrations, we would be able to capture useful toxicity signatures. These signitures may provide valuable mechanistic information. However, the 3R4F bPBS at the highest concentration tested was antiproliferative to B cells, T cells, coronary artery cells and fibroblasts in these systems. For HTP, HYB and EVP bPBS there were no anti-proliferative effects at any of the concentrations tested up to the maximal concentration of 1% in this study.

In contrast, previous studies have also investigated cytotoxicity following exposure of primary human bronchial epithelial cells to cigarette smoke or EVP aerosols. On the basis of the same smoking/puffing parameters and number of puffs, cell viability was about 4.5–5 times lower and the oxidative stress levels 4.5–5 times higher with combustible cigarettes (Scheffler et al., 2015). Further work using higher concentrations of cigarette smoke or NGP aerosol bPBS to find the cytotoxic doses of these products could be performed. However, given that the concentrations tested herein were already significantly higher than physiological levels, studies involving even higher concentrations may reduce the physiological relevance of any data produced.

Biomarker readout changes

The 3R4F bPBS demonstrated significant bioactivity in the BioMAP Diversity PLUS panel compared to HTP, HYB and EVP bPBS which, by contrast, showed minimal bioactivity. The 3R4F bPBS was active in 7 out of 12 cell systems with 22 Biomarkers annotated for significance. For 3R4F bPBS there was an increase in several acute inflammatory biomarkers including IL-1α, IL-8 and PGE2. There was also a decrease in biomarker levels of other proinflammatory and immunomodulatory biomarkers, (See Table 6) some of which have been reported to be elevated in the serum of smokers (Churg et al., 2004; Steeland et al., 2018; Barnes et al., 2011). The results presented here should not be compared directly to other cell systems and only carefully with human serum measurements. The key point is that BioMAP cell systems tested here are already under inflammatory stimulation, prior to exposure to the test compounds. Thus, they are already at increased levels in the

systems prior to adding the bPBS test articles. Depending on individual patient cohorts, changes in proinflammatory cytokines even in the serum may not change. Whilst this platform should not be used to directly to predict toxicity in humans, it is however, useful for the discovery of potential toxicity mechanisms.

Specific biomarkers altered for NGPs

The HTP, HYB and EVP bPBS altered ≤ 3 biomarkers with very small effect sizes compared to the 3R4F bPBS (See Fig. 1 and Table 5). It was notable that the NGP bPBS showed these weak effects even at concentrations that were approximately 8-fold higher than cigarette smoke bPBS (0.12% vs 1% concentrations). Lower levels of chemical constituents and of reduced complexity have been reported for HTP (Poussin et al., 2016) when compared to 3R4F in smoke. This was seen in terms on nicotine and carbonyls measured in this study (see Table 4).

Epidermal growth factor receptor (EGFR) is a growth factor receptor that induces cell differentiation and proliferation upon activation through the binding of one of its ligands. EGFR is thought to be involved the development of cancer, as the EGFR gene is often amplified, and/or mutated in cancer cells (Bethune et al., 2010). In this study, cell surface levels of EGFR in dermal fibroblasts were increased in 3R4F and, to a lesser extent in HYB bPBS-treated samples. Cigarette smoke has been previously observed to alter EGFR activation and impair EGFR degradation (Filosto et al., 2012). In contrast, EGFR levels were reduced in the HTP and EVP exposed samples, however, these were modest effects, only just outside of the control envelope.

M−CSF is a cytokine which causes hematopoietic stem cells to differentiate into macrophages or other related cell types. M−CSF levels were decreased by treatment with the 3R4F bPBS in peripheral blood and HUVECs co-cultures (LPS system) and by the HTP bPBS in the coronary artery smooth muscle cells. The overexpression of M−CSF is seen in many different cancer types, playing an important role in tumor vascularization, driving growth and differentiation of macrophages (Huang et al., 2014).

Cell surface levels of TF were increased in 3C and LPS cell systems following 3R4F bPBS exposure; these are linked to increased thrombin being released during thrombosis. TF is the primary cellular initiator of thrombosis and indeed, increased TF in the 3C system has been associated with drugs known to cause thrombosis-related side effects (Schamberger et al., 2015). Increased TF is also a characteristic of aryl hydrocarbon receptor (AhR) agonists (polycyclic aromatic hydrocarbons) (Kleinstreuer et al., 2014; Berg et al., 2015), and as such, this result is not unexpected due to the composition of cigarette smoke.

Cell surface thrombomodulin, was increased in cell system CASM3C by 3R4F bPBS exposed samples. Thrombomodulin has been reported to have anticoagulant, anti-inflammatory and cytoprotective activities during the process of fibrinolysis (Berg, 2019). However, these changes are not related to the BioMAP vascular toxicity signature, as this signature is restricted to the biology of vascular inflammation and smooth muscle cells that is associated with atherosclerosis, as described in (Berg, 2019).

The secreted form of interleukin 10 (sIL-10), an anti-inflammatory cytokine, was found to be modestly upregulated in HTP and EVP only in the macrophage and HUVECs. sIL-10 was decreased in 3R4F bPBS exposure in the macrophage and HUVECs. sIL10 is regulated by several pathways including EGFR. IL-10 is involved in T cell responses and modulates Th1-type responses to infection.

Specific biomarkers altered for 3R4F

The most affected assay system for 3R4F bPBS, with the larger observed magnitude of biomarker changes (decreases), was found to be the BT system, a model of T cell-dependent B cell activation (Melton et al., 2013) composed of B cells and peripheral blood mononuclear cells. This system is relevant for the development of allergy, asthma, autoimmunity, and oncology. This is the most sensi-

tive of the BioMAP cell systems and the observed result was expected from having both a longer culture time (3 and 6 days), and diversity (i.e. the greatest number) of possible detected mechanisms for modulating the immune system (Berg, 2017). In addition, the biomarkers measured in the BT system are exclusively in their soluble forms, with greater dynamic ranges as compared to cell-surface biomarker measurements. Across diverse compounds and substances, the BT system is the most frequently affected of the 12 cell systems, most likely due to the complexity and multiple ways it can be affected by chemicals.

Other biomarker changes of interest related to cardiovascular biology also warrant further study. For example, we observed that, in addition to triggering increased tissue factor in the LPS and 3C cell systems, treatment with 3R4F bPBS also triggered reductions in VCAM-1 in the HDF3CGF and LPS systems. VCAM-1 is an adhesion molecule involved in the recruitment of monocytes into sites of inflammation and is a clinical biomarker associated with cardiovascular disease and adhesion of monocytes the earliest stage of atherosclerosis (Postadzhiyan et al., 2008). While decreased VCAM could be considered a beneficial activity for cardiovascular disease processes, increased levels of TF through AhR activation in endothelial cells is potentially associated with thrombosis-related side effects *in vivo* (Berg et al., 2015). VCAM-1 is also the sentinel marker for nuclear factor erythroid 2-related factor 2 (NRF2), with decreased levels leading to potentially decreased oxidative stress (Kleinstreuer et al., 2014). Whether or not these mechanisms have any clinical relevance has yet to be determined.

More generally, clinical validation is critical for improving the utility of phenotypic assays such as BioMAP, for forecasting human outcomes and uncovering novel findings (Berg, 2017). Comparative analysis of the BioMAP profiles of test articles with the ones of known bioactive compounds in the reference database allows the identification of phenotypically similar compounds and provides insights into targets, possible MOAs and safety-related mechanisms (Berg et al., 2019).

Other applications of BioMap to complex mixtures

The use of BioMAP profiling depends on the reference database to make interpretations. It requires that a strong association between a particular biomarker activity and a particular clinical outcome be established. The systematic screening of single compounds and mixtures should help build a relevant database and can be compared to public reference data available from the ToxCast program (Houck et al., 2009; Kleinstreuer et al., 2014). The identification of human clinical biomarkers that may be reproducibly altered when an adult smoker uses an NGP as an alternative product versus an adult smoker that continues to exclusively smoke tobacco cigarettes, however, has been difficult due to only a limited number of biomarkers of effect being found for humans to date (Peck et al., 2018).

Indeed, whilst the human cell panel can provide mechanistic insights for single chemicals, the impact of mixtures, due to the complexity of biological systems, is more difficult to elucidate. In some cases, the activities induced by mixtures are additive of the individual components, but in other cases they can show synergistic or inhibitory interactions. In all cases, cellular feedback loops and adaptive mechanisms may also be present. Wetmore et al. (2019) analyzed the data from testing 30 fruit and vegetable extracts (complex mixtures) profiled through a subset of the BioMAP systems used here (8 of the 12 co-culture systems) and compared the results to the ToxCast chemicals (Wetmore et al., 2019). These extracts were chosen as humans are exposed to fruits and vegetables on a daily basis and they are considered to be 'safe'. The fruit and vegetable extracts were found to be quite active across the various BioMAP cell systems, and certain activities could be attributed to known bioactive substituents (e.g., tannic acid, polyphenols etc.) in the vegetable extracts. The authors state that high degree of bioactivity seen with the vegetable and fruit extracts

does not necessarily equate with an adverse response, as the appropriate comparison would be systemic exposure *in vivo* and not oral exposure (i.e. substances in the extracts must reach the systemic circulation and survive digestion and metabolic processing). The fruit and vegetable extracts had very different responses when compared to those for ToxCast chemicals when tested in BioMAP systems, with differences likely being related to both the complex mixture of chemicals in the produce extracts and the higher concentrations tested (Wetmore et al., 2019). This demonstrated that the BioMAP system can assess and screen complex mixtures as well as simple neat compounds in terms of biomarker changes/activity. It is not known if toxicity signatures have been applied to the vegetable extract data. The exposure of the BioMAP systems to bPBS trapped fractions of the 3R4F and NGPs may be more like systemic exposure *in vivo* as cells are not exposed directly to smoke/aerosol *in vivo* but to those constituents/fractions that can pass through the alveoli into the blood stream.

A reduction in VCAM-1, was seen for a number of extracts in Wetmore et al. (2019), is characteristic of nuclear factor kappa B (NF-κB) inhibition and NRF2 activation (Berg et al., 2010). Many natural products containing polyphenols reduce the level of VCAM-1, an observation that was also seen for the 3R4F bPBS. Cigarette smoke has been previously shown to stimulate the production of numerous pro-inflammatory cytokines including TNFα, IL-1, IL-6, IL-8 GM-CSF and to decrease the levels of anti-inflammatory cytokines such as IL-10 (Arnson et al., 2010). Whilst some of these changes were seen with 3R4F bPBS in BioMAP profiling (increased IL-8, IL-1, decreased IL10) some cytokines were decreased including TNFα, IL-6 and M−CSF possibly reflecting differences in cytokine responses in cultured cells vs *in vivo* tissues (Arnson et al., 2010), but more likely relating to the different tissue contexts. Cytokine levels in BioMAP systems are already induced by activators (e.g., cytokines, TLR ligands or TCR ligands).

Analysis of data for the toxicity signatures

The analysis of the BioMAP Diversity PLUS profile data for Toxicity Signatures sets of biomarkers associated with specific pharmacological responses or adverse effects (Berg, 2019) revealed that only 3R4F bPBS demonstrated any of the nine signatures. Three signatures were identified, thrombosis (at ≥ 0.12%), skin irritation (≥ 0.25%), and immunosuppression (≥ 0.25%). As 3R4F was not tested at concentrations lower than 0.12%, the lowest active concentration was not determined for the thrombosis signature. Overall, NGP product materials were less active with fewer numbers of biomarkers altered (none of which were unique/novel to the NGPs when compared to 3R4F) with modest effect sizes (i.e. limited change from the control envelope), and no toxicity signatures were observed for data derived from testing these materials. As each of the toxicity signatures required 2–5 biomarkers to make up the signature, the lack of toxicity signatures identified for all the NGPs at 1% was not unexpected due to the lack of biomarkers altered by the NGPs in BioMap and the close proximity of the minimally biomarkers changes to the control (grey central envelope in Figure 1).

Smoking has been shown to modulate various aspects of immune systems for both the adaptive and innate systems, altering the development of cells and their function, with some aspects of immunosuppression in T-cell populations (Arnson et al., 2010; Qiu et al., 2017). Immunosuppression in toxicity signatures is defined as increased likelihood of infection in humans. Five biomarkers make up this signature, with decreased T cell proliferation in the BioMAP SAg system as the key biomarker activity (Berg, 2019). Immunosuppressive agents such as sirolimus, infliximab, cyclosporine, tacrolimus, mycophenolate and azathioprine share this signature which is associated with the following mechanisms: mechanistic target of rapamycin (mTOR), calcineurin, Janus kinase, Heat shock protein 90, nuclear factor of

activated T cells and DNA proliferation as targets or pathways involved. The clinical mechanism implicated by this signature is depressed responses of immune cells (Berg, 2019). This finding was not unexpected for cigarette smoke extracts. One of the mechanisms driving immunomodulation has been identified as the activation of the AhR receptor (Wang et al., 2019). The BioMAP platform has successfully been used to implicate the AhR pathway in skin toxicity (Shah et al., 2017). Smoking has been linked to atopic conditions such as hand eczema (Molin et al., 2015), as well as increasing the response to immunotherapy in oncology via the AhR receptor (Wang et al., 2019). There are several potential aromatic hydrocarbons that are naturally occurring in tobacco smoke and commonly measured smoke analytes (Jaccard et al., 2019).

For the thrombosis signature the AhR receptor was also identified as a possible underlying mechanism and could be activated by aromatic hydrocarbons trapped in the bPBS. Whilst we did not measure AhR directly trapped in bPBS, several authors have previously trapped cigarette smoke in 20 mL of serum-free minimum essential medium at a rate of 1 cigarette/min. Exposure of human lung fibroblasts to 2% cigarette smoke extract showed moderate AhR nuclear localization at 15 min. After a 2-h exposure to cigarette smoke extract, there was almost exclusive and strong nuclear staining. These findings indicated that the AhR was activated by components of cigarette smoke extract binding to the AhR, inducing translocation to the nucleus (Martey et al., 2005; Baglole, 2008).

The toxicity signature for thrombosis is described as the increased likelihood of stroke, deep vein thrombosis or pulmonary embolism. Three biomarkers make up this signature, with increased TF/CD142 in the BioMAP 3C system as the key biomarker (Berg, 2019; Berg et al., 2015). This signature is exhibited by drugs associated with increased incidence of thrombosis related side effects including sirolimus, crizotinib, raloxifene, tamoxifen and clozapine, as well as aryl hydrocarbons, selective estrogen receptor modulators and antipsychotics. Target mechanisms associated with this signature include mTOR, AhR, V-ATPase, lysosomal function, CYP17A, PKC, NOD2, estrogen receptor, H1R, HIF-1α, thyroid hormone receptor and the Oncostatin M receptor. The clinical mechanism implicated is vascular autophagy that leads to increased thrombotic potential within the vasculature. Cigarette smoking has previously been associated with thrombosis due to the observation of increased levels of clotting factors, vascular inflammation, and is seen as a common complication in COPD patients (Tapson, 2005). These endpoints were not detectable for any of the NGPs despite increased nicotine delivery to the system when compared to 3R4F. There was no increase in serum amyloid A in the CASM3C system for any of the NGPs or 3R4F, which is the sentinel marker of the vascular toxicity signature. Note that this signature represents only certain mechanisms associated with vascular inflammation and atherosclerosis.

The toxicity signature for skin irritation is defined by increased likelihood of irritation of the skin with reddening and itch. Three biomarkers make up this signature, with increased PGE$_2$ in the BioMAP LPS system as the key biomarker activity (Berg, 2019). Irritants including retinoic acid, retinol, vitamin D, ritonavir, imatinib, 2-chloroethyl ethyl sulphide and calcitriol all share this signature which has been identified with retinoids, vesicants and blister agents and the following target pathway mechanisms: retinoid acid receptor/ retinoid X receptor, AhR and vitamin D3 receptor VDR (Shah et al., 2017). The clinical mechanism implicated is sustained production of prostaglandins leading to vascular permeability, leukocyte infiltration and promotion of Th17 responses.

The signature for vascular toxicity was not indicated due to the lack of biomarker changes in the two key biomarkers indicative of vascular toxicity within this assay. This, as stated above may also reflect the fact that cells are already stimulated prior to exposure and the inflammatory changes due to the addition of 3R4F bPBS were not sufficient to leave the control envelope for these key biomarkers. However, it

should be noted that cigarette TPM, when tested at higher concentrations, does flag for multiple toxicity signatures including vascular toxicity, without overt cytotoxicity. This information is included in the Supplemental Materials (Supplementary Figs. 1 and 2).

A review of the BioMAP profiles of 776 individual ToxCast chemicals analyzed for toxicity signatures, of which almost all are individual chemicals (Berg et al., 2019), found that the most frequently identified signatures were immunosuppression (279); organ toxicity (269) and skin sensitization (180). Cigarette smoke is a complex mixture (>7000 compounds measured in smoke (Rodgman and Perfetti, 2013), compared to the reduced levels and/or numbers of constituents measured in HTP (Li et al., 2019) HYB and EVP, which is probably why 3R4F bPBS was active in multiple (7) cell systems compared to minimal effects seen with HTP, suggesting that the many different smoke constituents may be responsible for potentially increased mechanisms of toxicity. These findings are also in line with the general harm risk reduction continuum, with NGPs having significantly reduced effects when compared to combustible cigarettes (McNeill et al., 2015).

Study limitations

A possible limitation to the current study is the lack of liver model or means to achieve metabolic activation, to assess the formation of secondary metabolites. However, the currently formatted panel of BioMAP assays do represent what cells are likely to be exposed to *in vivo* in the blood plasma prior to any metabolic activation/ detoxification by the liver (first pass metabolism).

The toxicity signatures described here also are not comprehensive. They are mechanism-based and capture some of the mechanisms for each of the categories, but do not necessarily capture all possible acting mechanisms. The absence of a toxicity signature should not be interpreted to mean that the test article is safe. If a Toxicity Signature is observed for one test article, but not another, it may indicate that a particular mechanism related to for example vascular toxicity outcomes is present in one test article, but not the other (See Supplemental data Table 1, for the key biomarkers and mechanisms captured under each signature). However, theses signatures were based on adverse events in clinical trials for a reference data base of >4500 compounds. In addition to test article screening using the BioMAP system, further mechanistic studies, such as high content screening and 3D models, should also be used for the *in vitro* toxicity assessment of NGPs compared to cigarettes using a weight of evidence approach.

One limitation is uncertainty in how exposures in smokers (prolonged exposures) compare with the short term exposures tested here. Smoking related diseases develop over decades and cannot be replicated with *in vitro* assays. With this caveat, we can compare the relative cellular effects between the different test article exposures. Lung epithelial cells may not receive all of the dose due to the absorption of highly reactive carbonyls in the upper respiratory tract, as these are compounds are both highly unstable being chemically short lived and are very soluble in water. Formaldehyde, a highly reactive and water soluble vapor, was estimated to be taken up by the tissues in the upper tracheobronchial airways with only limited penetration into the lung. However, carbonyls with moderate solubility such as acetaldehyde and acrolein and were predicted to penetrate deeper into the lung, reaching the alveolar region. Here the absorbed carbonyls have a much higher probability of passing through the thin alveolar-capillary membrane to reach the blood and the circulatory system (Asgharian et al., 2012). Seeman et al. (2002) reported mainstream smoke acetaldehyde deposited primarily in the upper respiratory tract, including the mouth, of the smoker, and any acetaldehyde is rapidly metabolized by aldehyde dehydrogenase in the blood and elsewhere in the body, being unlikely to be available to secondary tissues (Seeman et al., 2002). In addition, the dose once in the circulatory systems to secondary tissues will likely be considerably lower due to the

effects of both dilution in the blood and possible metabolism and removal by the liver or other tissues. However, the surface area of the lung is also considerable with the tracheal bronchi region having a surface area of approximately 2471 ± 320 cm^2 (Mercer et al., 1994), with the surface area of the alveolar surface area was estimated to be 143 (± 12)m^2 on the average (Gehr et al., 1978), so the dose per unit surface area of the lung is potentially reduced when compared to the surface area of this system. Finally, another limitation of this study is that using submerged cultures for the bPBS test articles, may result in different tissues exposures being seen under real life conditions (*in vivo*). The same concentration were used across the 12 test systems, this may not fully represent the *in vivo* situation. Whilst this is a limitation, the results of this study are useful in identifying biomarker activities in specific tissue contexts that can be further evaluated in additional translational studies, and thereby try to establish the relationship between sample concentrations and potential *in vivo* effects.

Conclusion

In this study, we compared the response profiles of a series of complex mixtures including 3R4F reference cigarette smoke and three different types of commercially available NGPs, using aerosol or smoke bPBS, in 12 human primary cell-based systems (BioMAP Diversity PLUS panel). Samples were applied directly to the BioMAP systems at concentrations typically above those considered to be physiologically relevant (between 2 and 152 times the peak nicotine concentrations measured in the plasma of smokers and EVP users). The 3R4F bPBS at the maximum concentration of 1% showed the greatest numbers of altered biomarkers (22 of 148) compared to the NGP bPBS samples (≤ 3) tested at 1%. Analysis of the data for toxicity signatures showed that 3R4F bPBS extracts demonstrated toxicity signatures for immunosuppression ($\geq 0.25\%$), thrombosis ($\geq 0.12\%$) and skin irritation ($\geq 0.25\%$). Data from testing NGP samples did not demonstrate any toxicity signatures at 1% under the conditions of test.

This initial screen indicated reduced toxicity of NGPs when compared to a combusted product, in line with the hypothesized tobacco nicotine continuum (McNeill and Munafò, 2013; Institute of Medicine, 2001). However, the long term risk would need to be substantiated in human clinical studies. This assay is a useful screening tool for rapid product comparison purposes with multiple human primary cell types. As such when used with other assays the BioMAP system can be used as part of a weight of evidence approach for examining the reduced risk potential of NGPs.

CRediT authorship contribution statement

Declaration of Competing Interest

Appendix A. Supplementary data

Supplementary data to this article can be found online at https://doi.org/10.1016/j.crtox.2021.08.003.

References

Adamson, J. et al, 2017. Nicotine quantification in vitro: a consistent dosimetry marker for e-cigarette aerosol and cigarette smoke generation. Appl. In Vitro Toxicol. 3 (1), 14–27.

Arnson, Y., Shoenfeld, Y., Amital, H., 2010. Effects of tobacco smoke on immunity, inflammation and autoimmunity. J. Autoimmun. 34 (3), J258–J265.

Asgharian, B., Price, O.T., Schroeter, J.D., Kimbell, J.S., Singal, M., 2012. A lung dosimetry model of vapor uptake and tissue disposition. Inhal. Toxicol. 24 (3), 182–193.

Baglole, C.J. et al, 2008. The aryl hydrocarbon receptor attenuates tobacco smoke-induced cyclooxygenase-2 and prostaglandin production in lung fibroblasts through regulation of the NF-kappaB family member RelB. J. Biol. Chem. 283 (43), 28944–28957.

Barnes, T.C., Anderson, M.E., Moots, R.J., 2011. The many faces of interleukin-6: the role of IL-6 in inflammation, vasculopathy, and fibrosis in systemic sclerosis. Int. J. Rheumatol. 2011, 721608.

Behrsing, H. et al, 2018. Characterization of a Vitrocell VC1 using nicotine dosimetry: an essential component toward standardized in vitro aerosol exposure of tobacco and next generation nicotine delivery products. Appl. In Vitro Toxicol. 4 (2), 159–166.

Benowitz, N.L., Hukkanen, J., Jacob 3rd, P., 2009. Nicotine chemistry, metabolism, kinetics and biomarkers. Handb. Exp. Pharmacol. 192, 29–60.

Berg, E.L., 2017. Phenotypic chemical biology for predicting safety and efficacy. Drug Discovery Today: Technol. 23, 53–60.

Berg, E.L., 2019. Human cell-based in vitro phenotypic profiling for drug safety-related attrition. Front. Big Data 2 (47).

Berg, E.L., et al. Evaluation of EPA's ToxCast Data from the BioMAP® Platform for Human-Relevant Toxicity Signatures. 2019; Available from: https://www.discoverx.com/tools-resources/document-resource-library/documents/sot-2019-biomap-toxicology-poster.

Berg, E., Polokoff, M., O'Mahony, A., Nguyen, D., Li, X., 2015. Elucidating mechanisms of toxicity using phenotypic data from primary human cell systems–a chemical biology approach for thrombosis-related side effects. Int. J. Mol. Sci. 16 (1), 1008–1029.

Berg, E.L., Yang, J., Melrose, J., Nguyen, D., Privat, S., Rosler, E., Kunkel, E.J., Ekins, S., 2010. Chemical target and pathway toxicity mechanisms defined in primary human cell systems. J. Pharmacol. Toxicol. Methods 61 (1), 3–15.

Berg, E.L., Yang, J., Polokoff, M.A., 2013. Building predictive models for mechanism-of-action classification from phenotypic assay data sets. J. Biomol. Screen. 18 (10), 1260–1269.

Bethune, G. et al, 2010. Epidermal growth factor receptor (EGFR) in lung cancer: an overview and update. J. Thorac Dis. 2 (1), 48–51.

Brossard, P., Weitkunat, R., Poux, V., Lama, N., Haziza, C., Picavet, P., Baker, G., Lüdicke, F., 2017. Nicotine pharmacokinetic profiles of the Tobacco Heating System 2.2, cigarettes and nicotine gum in Japanese smokers. Regul. Toxicol. Pharm. 89, 193–199.

Buratto, R. et al, 2018. Determination of eight carbonyl compounds in aerosols trapped in phosphate buffer saline solutions to support in vitro assessment studies. Talanta 184, 42–49.

Churg, A. et al, 2004. Tumor necrosis factor-alpha drives 70% of cigarette smoke-induced emphysema in the mouse. Am. J. Respir. Crit. Care Med. 170 (5), 492–498.

Czekala, L. et al, 2019. Toxicological comparison of cigarette smoke and e-cigarette aerosol using a 3D in vitro human respiratory model. Regul. Toxicol. Pharm. 103, 314–324.

Czekala, L., et al., 2021, The in vitro ToxTracker and Aneugen Clastogen Evaluation extension assay as a tool in the assessment of relative genotoxic potential of e-liquids and their aerosols. Mutagenesis.

Farsalinos, K. et al, 2013. Comparison of the cytotoxic potential of cigarette smoke and electronic cigarette vapour extract on cultured myocardial cells. Int. J. Environ. Res. Public Health 10 (10), 5146–5162.

Filosto, S., Becker, C.R., Goldkorn, T., 2012. Cigarette smoke induces aberrant EGF receptor activation that mediates lung cancer development and resistance to tyrosine kinase inhibitors. Mol. Cancer Ther. 11 (4), 795–804.

Gasparyan, H. et al, 2018. Accurate measurement of main aerosol constituents from heated tobacco products (HTPs): implications for a fundamentally different aerosol. Regul. Toxicol. Pharm. 99, 131–141.

Gehr, P., Bachofen, M., Weibel, E.R., 1978. The normal human lung: ultrastructure and morphometric estimation of diffusion capacity. Respir. Physiol. 32 (2), 121–140.

Goniewicz, M.L. et al, 2014. Levels of selected carcinogens and toxicants in vapour from electronic cigarettes. Tob Control 23 (2), 133–139.

Hartung, T., 2016. E-cigarettes and the need and opportunities for alternatives to animal testing. Altex 33 (3), 211–224.

Houck, K.A. et al, 2009. Profiling bioactivity of the ToxCast chemical library using BioMAP primary human cell systems. J. Biomol. Screen. 14 (9), 1054–1066.

Huang, L., Xu, X., Hao, Y., 2014. The possible mechanisms of tumor progression via CSF-1/CSF-1R pathway activation. Rom. J. Morphol. Embryol. 55 (2 Suppl), 501–506.

Institute of Medicine, Clearing the Smoke: Assessing the Science Base for Tobacco Harm Reduction, ed. K. Stratton, et al. 2001, Washington, DC: The National Academies Press. 656.

International Organization for Standardization, ISO 3402:1999, in Tobacco and tobacco products — Atmosphere for conditioning and testing. 1999: https://www.iso.org/standard/28324.html. p. 5.

ISO, I.O.f.S., ISO 21160:2018 Cigarettes — Determination of selected carbonyls in the mainstream smoke of cigarettes — Method using high performance liquid chromatography. 2018.

Jaccard, G., Djoko, D.T., Korneliou, A., Stabbert, R., Belushkin, M., Esposito, M., 2019. Mainstream smoke constituents and in vitro toxicity comparative analysis of 3R4F and 1R6F reference cigarettes. Toxicol. Rep. 6, 222–231.

Johnson, M.D., Schilz, J., Djordjevic, M.V., Rice, J.R., Shields, P.G., 2009. Evaluation of in vitro assays for assessing the toxicity of cigarette smoke and smokeless tobacco. Cancer Epidemiol. Biomarkers Prev. 18 (12), 3263–3304.

Kleinstreuer, N.C. et al, 2014. Phenotypic screening of the ToxCast chemical library to classify toxic and therapeutic mechanisms. Nat. Biotechnol. 32 (6), 583–591.

Krewski, D. et al, 2010. Toxicity testing in the 21st century: a vision and a strategy. J. Toxicol. Environ. Health B Crit. Rev. 13 (2–4), 51–138.

Li, X., et al., 2019, Chemical Analysis and Simulated Pyrolysis of Tobacco Heating System 2.2 Compared to Conventional Cigarettes. Nicotine Tob Res, 21(1): p. 111-118.

Martey, C.A., Baglole, C.J., Gasiewicz, T.A., Sime, P.J., Phipps, R.P., 2005. The aryl hydrocarbon receptor is a regulator of cigarette smoke induction of the cyclooxygenase and prostaglandin pathways in human lung fibroblasts. Am. J. Physiol. Lung Cell. Mol. Physiol. 289 (3), L391–L399.

Mathis, C. et al, 2013. Systems biology approach reveals a dose-dependent recovery of primary human airway epithelium culture after exposure to cigarette smoke. Toxicol. Lett. 221, S196.

A, M., et al. E-cigarettes: an evidence update A report commissioned by Public Health England. 2015; Available from: https://assets.publishing.service.gov.uk/government/uploads/system/uploads/attachment_data/file/733022/Ecigarettes_an_evidence_update_A_report_commissioned_by_Public_Health_England_FINAL.pdf.

McNeill, A., Munafò, M.R., 2013. Reducing harm from tobacco use. J. Psychopharmacol. 27 (1), 13–18.

Melton, A.C., Melrose, J., Alajoki, L., Privat, S., Cho, H., Brown, N., Plavec, A.M., Nguyen, D., Johnston, E.D., Yang, J., Polokoff, M.A., Plavec, I., Berg, E.L., O'Mahony, A., Fritz, J.H., 2013. Regulation of IL-17A Production Is Distinct from IL-17F in a Primary Human Cell Co-culture Model of T Cell-Mediated B Cell Activation. PLoS ONE 8 (3), e58966.

Mercer, R.R., Russell, M.L., Roggli, V.L., Crapo, J.D., 1994. Cell number and distribution in human and rat airways. Am. J. Respir. Cell Mol. Biol. 10 (6), 613–624.

Misra, M. et al, 2014. Comparative in vitro toxicity profile of electronic and tobacco cigarettes, smokeless tobacco and nicotine replacement therapy products: e-liquids, extracts and collected aerosols. Int. J. Environ. Res. Public Health 11 (11), 11325–11347.

Molin, S., Ruzicka, T., Herzinger, T., 2015. Smoking is associated with combined allergic and irritant hand eczema, contact allergies and hyperhidrosis. J. Eur. Acad. Dermatol. Venereol. 29 (12), 2483–2486.

National Academies of Sciences, E., et al., in Using 21st Century Science to Improve Risk-Related Evaluations. 2017, National Academies Press (US) Copyright 2017 by the National Academy of Sciences. All rights reserved.: Washington (DC).

O'Connell, G. et al, 2019. A randomised, open-label, cross-over clinical study to evaluate the pharmacokinetic profiles of cigarettes and e-cigarettes with nicotine salt formulations in US adult smokers. Intern. Emerg. Med. 14 (6), 853–861.

O'Mahony, A., et al., 2018, AB0050 Biomap® phenotypic profiling of two batches of originator etanercept reveals equivalent activity signatures consistent with conserved biological activity. Vol. 77. 1225.1-1225.

Peck, M.J., Sanders, E.B., Scherer, G., Lüdicke, F., Weitkunat, R., 2018. Review of biomarkers to assess the effects of switching from cigarettes to modified risk tobacco products. Biomarkers 23 (3), 213–244.

Plus, E.D. BioMAP Diversity PLUS Panel. 2021 [cited 2021 5th May]; Available from: https://www.eurofinsdiscoveryservices.com/services/phenotypic-assays/biomap/diversity-plus/.

Polosa, R. et al, 2017. Health impact of E-cigarettes: a prospective 3.5-year study of regular daily users who have never smoked. Sci. Rep. 7 (1). https://doi.org/10.1038/s41598-017-14043-2.

Postadzhiyan, A.S., Tzontcheva, A.V., Kehayov, I., Finkov, B., 2008. Circulating soluble adhesion molecules ICAM-1 and VCAM-1 and their association with clinical outcome, troponin T and C-reactive protein in patients with acute coronary syndromes. Clin. Biochem. 41 (3), 126–133.

Poussin, C., Laurent, A., Peitsch, M.C., Hoeng, J., De Leon, H., 2016. Systems toxicology-based assessment of the candidate modified risk tobacco product THS2.2 for the adhesion of monocytic cells to human coronary arterial endothelial cells. Toxicology 339, 73–86.

Pratte, P., Cosandey, S., Goujon Ginglinger, C., 2017. Investigation of solid particles in the mainstream aerosol of the Tobacco Heating System THS2.2 and mainstream smoke of a 3R4F reference cigarette. Hum. Exp. Toxicol. 36 (11), 1115–1120.

Qiu, F. et al, 2017. Impacts of cigarette smoking on immune responsiveness: Up and down or upside down? Oncotarget 8 (1), 268–284.

Rodgman, A., Perfetti, T.A., 2013. The Chemical Components of Tobacco and Tobacco Smoke, Second Edition. 2nd ed., CRC Press, Boca Raton.

Schamberger, A.C., Staab-Weijnitz, C.A., Mise-Racek, N., Eickelberg, O., 2015. Cigarette smoke alters primary human bronchial epithelial cell differentiation at the air-liquid interface. Sci. Rep. 5 (1). https://doi.org/10.1038/srep08163.

Scheffler, S. et al, 2015. Evaluation of E-cigarette liquid vapor and mainstream cigarette smoke after direct exposure of primary human bronchial epithelial cells. Int. J. Environ. Res. Public Health 12 (4), 3915–3925.

Schneider, N.G. et al, 2001. The nicotine inhaler: clinical pharmacokinetics and comparison with other nicotine treatments. Clin. Pharmacokinet. 40 (9), 661–684.

Seeman, J.I., Dixon, M., Haussmann, H.J., 2002. Acetaldehyde in mainstream tobacco smoke: formation and occurrence in smoke and bioavailability in the smoker. Chem. Res. Toxicol. 15 (11), 1331–1350.

Shah, F., Stepan, A.F., O'Mahony, A., Velichko, S., Folias, A.E., Houle, C., Shaffer, C.L., Marcek, J., Whritenour, J., Stanton, R., Berg, E.L., 2017. Mechanisms of skin toxicity associated with metabotropic glutamate receptor 5 negative allosteric modulators. Cell Chem. Biol. 24 (7), 858–869.e5.

Sheldon, L.S., Cohen Hubal, E.A., 2009. Exposure as part of a systems approach for assessing risk. Environ. Health Perspect. 117 (8), 1181–1194.

Simms, L. et al, 2020. The use of human induced pluripotent stem cells to screen for developmental toxicity potential indicates reduced potential for non-combusted products, when compared to cigarettes. Curr. Res. Toxicol. 1, 161–173.

Smart, D.J., Phillips, G., 2021. Collecting e-cigarette aerosols for in vitro applications: a survey of the biomedical literature and opportunities to increase the value of submerged cell culture-based assessments. J. Appl. Toxicol. 41 (1), 161–174.

Standardization, I.O.f. ISO 20778:2018 Cigarettes — Routine analytical cigarette smoking machine — Definitions and standard conditions with an intense smoking regime. 2018 [cited 2020 15th September]; Available from: https://www.iso.org/standard/69065.html.

Standardization, I.O.f. ISO 20768:2018 Vapour products — Routine analytical vaping machine — Definitions and standard conditions. 2018 [cited 2020 15th September]; Available from: https://www.iso.org/standard/69019.html.

Steeland, S., Libert, C., Vandenbroucke, R.E., 2018. A new venue of TNF targeting. Int. J. Mol. Sci. 19 (5), 1442.

Tapson, V.F., 2005. The role of smoking in coagulation and thromboembolism in chronic obstructive pulmonary disease. Proc. Am. Thorac. Soc. 2 (1), 71–77.

Taylor, M. et al, 2020. In vitro biological assessment of the stability of cigarette smoke aqueous aerosol extracts. BMC Res. Notes 13 (1), 492.

Walele, T. et al, 2018. Evaluation of the safety profile of an electronic vapour product used for two years by smokers in a real-life setting. Regul. Toxicol. Pharm. 92, 226–238.

Wang, G.-Z., Zhang, Li., Zhao, X.-C., Gao, S.-H., Qu, L.-W., Yu, H., Fang, W.-F., Zhou, Y.-C., Liang, F., Zhang, C., Huang, Y.-C., Liu, Z., Fu, Y.-X., Zhou, G.-B., 2019. The Aryl hydrocarbon receptor mediates tobacco-induced PD-L1 expression and is associated with response to immunotherapy. Nat. Commun. 10 (1), 1125.

Wetmore, B.A. et al, 2019. Assessing bioactivity-exposure profiles of fruit and vegetable extracts in the BioMAP profiling system. Toxicol. In Vitro 54, 41–57.

WHO, 2019. WHO report on the global tobacco epidemic 2019: offer help to quit tobacco use. Available from: https://www.who.int/teams/health-promotion/tobacco-control/who-report-on-the-global-tobacco-epidemic-2019&publication=9789241516204.

Zhu, S.-H. et al, 2014. Four hundred and sixty brands of e-cigarettes and counting: implications for product regulation. Tob Control 23 (suppl 3), iii3–iii9.